Numerical analysis of spectra of the Frobenius-Perron operator of a noisy one-dimensional mapping: Toward a theory of stochastic bifurcations

Junko Inoue,[1] Shinji Doi,[2,*] and Sadatoshi Kumagai[2]
[1]*Faculty of Human Relation, Koka Women's University, Kyoto 615, Japan*
[2]*Department of Electrical Engineering, Graduate School of Engineering, Osaka University, Osaka 565-0871, Japan*
(Received 15 May 2001; published 23 October 2001)

A different method to detect the stochastic bifurcation point of a one-dimensional mapping in the presence of noise is proposed. This method analyzes the eigenvalues and eigenfunctions of the noisy Frobenius-Perron operator. The invariant density or the eigenfunction of the eigenvalue 1 of the operator possesses ''static'' information of the noisy one-dimensional dynamics while the other eigenvalues and eigenfunctions have ''dynamic'' information. Clear bifurcation phenomena have been observed in a noisy sine-circle map and both stochastic saddle-node and period-doubling bifurcation points have been successfully defined in terms of the eigenvalues.

DOI: 10.1103/PhysRevE.64.056219 PACS number(s): 05.45.−a, 02.30.Oz, 02.50.Fz, 05.40.Ca

I. INTRODUCTION

One-dimensional (1D) mappings or one-dimensional discrete-time dynamical systems have been intensively studied and used to model various nonlinear phenomena [1,2]. The effects of noise on 1D mappings have also been investigated by various researchers since the real physical system cannot avoid such noise [3–8]. 1D mappings present several bifurcations such as tangent (or saddle-node) and flip (or period-doubling) bifurcations in the noise-free case. What happens in the bifurcation phenomena if noise is added? Noise may just blur the critical bifurcation.

The 1D maps with chaotic dynamics are studied in terms of the invariant density of the Frobenius-Perron (FP) operator of the map. A noisy 1D map can also be studied by the invariant density of the ''noisy'' FP operator [9]. The invariant density of the noisy FP operator denotes a stationary distribution of a variable. A classical definition of a stochastic bifurcation in noisy dynamical systems is based on the change of topological shapes of the invariant densities [6] and lacks the dynamic information of a system [10]. In fact, we cannot see any critical change in the shapes of the invariant densities near saddle-node bifurcation points of the deterministic 1D mapping studied in the present paper. Recent development of a stochastic bifurcation theory overcomes the drawback and takes the dynamical information of a stochastic system into account [10]. Since *the theory of stochastic bifurcation is still in its infancy* [10] in spite of the recent big progress of the theory of random dynamical systems, more intensive researches are necessary for the establishment of the stochastic bifurcation theory.

We have proposed a method that uses spectra (eigenvalues) of an operator that governs the probability density evolution of a system and shown that this method is useful to detect stochastic phase lockings (saddle-node bifurcations) using the noisy van der Pol oscillator driven by a periodic signal [11]. Since the previous study treated stochastic saddle-node bifurcations only, the present paper considers both saddle-node and period-doubling bifurcations using the simpler dynamical system (1D mapping) and discusses the validity and the applicability of our method to both the bifurcations in detail.

The present paper is organized as follows. Section II shows the mathematical framework to treat noisy 1D mappings. Our method that uses the spectra of the Frobenius-Perron operator is applied to the saddle-node bifurcations in a noisy sine-circle mapping in Sec. III. Section IV extends the method to the case of period-doubling bifurcations and discusses the validity and difficulty in detail and the paper concludes with some brief comments in Sec. V.

II. STOCHASTIC KERNEL AND THE FROBENIUS-PERRON OPERATOR

We consider a 1D discrete-time dynamical system defined on a unit circle S in the presence of additive noise:

$$X_{n+1}=f(X_n)+\xi_n, \quad X_n\in S \quad n=0,1,2,\ldots, \tag{1}$$

where $\xi_0,\ldots,\xi_n$ are independent random variables with an identical probability density function g.

Define a kernel function $k(x_0,x_1)$ using a conditional probability density function,

$$k(x_0,x_1)dx_1=\Pr\{x_1\leqslant X_{n+1}\leqslant x_1+dx_1|X_n=x_0\}. \tag{2}$$

As is easily seen from this definition, the function k has the property

$$k(x_0,x_1)\geqslant 0, \quad \int_S k(x_0,x_1)dx_1=1 \tag{3}$$

and is called a stochastic kernel. Since $\xi_0,\ldots,\xi_n$ are mutually independent and have the same density g, it is easy to show that

*Author to whom correspondence should be addressed. Email address: doi@pwr.eng.osaka-u.ac.jp

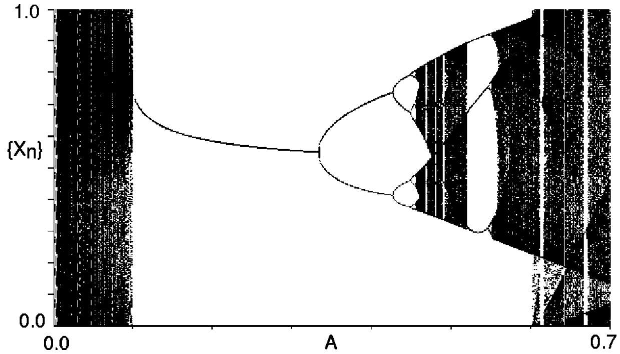

FIG. 1. Deterministic bifurcation diagram of the sine-circle map (7). The bifurcation parameter is the amplitude A and the value of t is fixed to 0.1. Asymptotic sequences $\{X_n\}$, $n=201,\ldots,700$ produced by Eq. (1) were plotted for each of 1000 equally spaced A values on the interval $[0,0.7]$ when $\xi\equiv 0$.

$$k(x_0,x_1)=g(x_1-f(x_0)).$$

Using the kernel function k, the FP operator [8,9,13] on $\mathcal{D}$ in the presence of noise is defined by:

$$\mathcal{P}h(x)=\int_S k(x_0,x)h(x_0)dx_0,$$

$$=\int_S g(x-f(x_0))h(x_0)dx_0,\quad h\in\mathcal{D} \tag{4}$$

where $\mathcal{D}$ is the set of absolutely integrable non-negative functions with a unit L^1 norm on S. Let $h_0\in\mathcal{D}$ denote the probability density function of the initial state X_0. Then the density function h_1 of the state X_1 at the next time is obtained by $h_1(x)=\mathcal{P}h_0(x)$. The density function at the nth time is also obtained by

$$h_n(x)=\mathcal{P}h_{n-1}(x)=\cdots=\mathcal{P}^n h_0(x). \tag{5}$$

A function $h^*(x)$ is called as the invariant density function of the operator $\mathcal{P}$ if the relation $\mathcal{P}h^*=h^*$ holds. The invariant density is *asymptotically stable* if for any initial density function $h_0\in\mathcal{D}$

$$\lim_{n\to\infty}||\mathcal{P}^n h_0-h^*||=0.$$

Furthermore, the operator has a unique asymptotically stable invariant density if the kernel function k satisfies the inequality [9]

$$\int_S \inf_{x_0} k(x_0,x_1)dx_1>0. \tag{6}$$

Numerically, this linear operator $\mathcal{P}$ is expressed in a discrete form (matrix). In the below we analyzes the spectral properties of the matrix. Note that we have done several numerical computation with different discretization sizes of the operator and confirmed ourselves that the following numerical results do not depend on the discretization size.

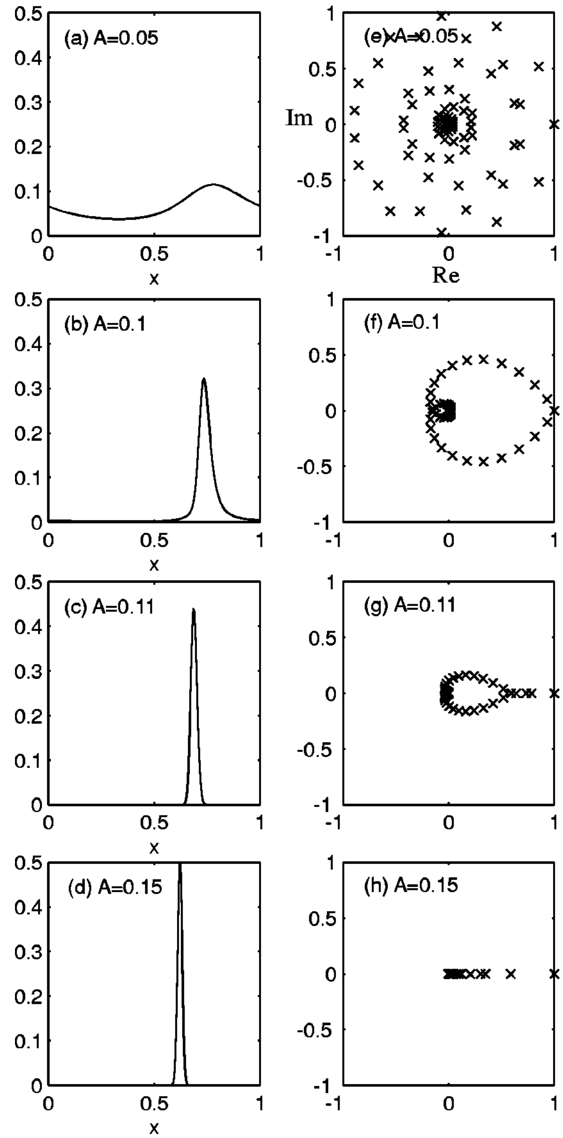

FIG. 2. Stochastic saddle-node bifurcation. Invariant densities and whole spectra of the FP operator $\mathcal{P}$ are plotted, where $t=0.1$ and $\sigma=0.01$. (a)–(d): Invariant densities $h^*(x)$ of $\mathcal{P}$. (e)–(h): Eigenvalues of the operator $\mathcal{P}$. The abscissa and the ordinate are the real part and imaginary part of the eigenvalues in (e)–(h). The operator $\mathcal{P}$ is approximated by an $n\times n$ matrix, where $n=200$. In a deterministic case, the saddle-node bifurcation from quasiperiodic to period 1 occurs exactly at $A=0.10$. Corresponding stochastic bifurcation occurs between $A=0.10$ [(b) and (f)] and $A=0.11$ [(c) and (g)].

III. SINE-CIRCLE MAP IN THE PRESENCE OF ADDITIVE NOISE

We consider a sine-circle map on S as a typical 1D map,

$$f(x)=x+A\sin(2\pi x)+t,\quad \mathrm{mod}\,1. \tag{7}$$

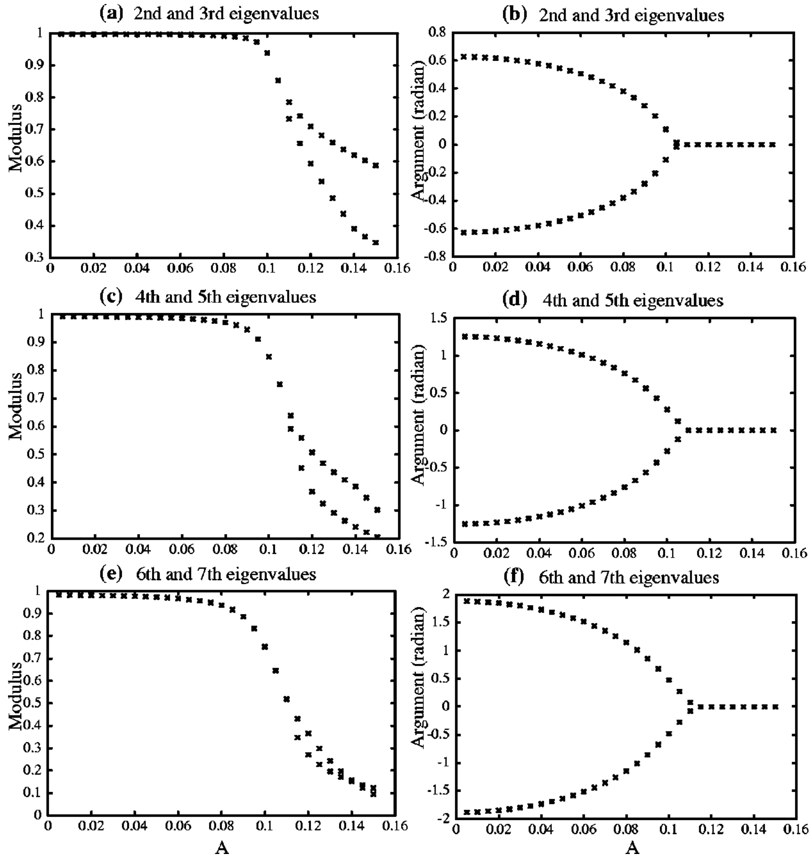

FIG. 3. Spectral bifurcation diagram of stochastic saddle-node bifurcation. Moduli and angles (arguments in radians) of the second, third, fourth, fifth, sixth, and seventh eigenvalues of the operator $\mathcal{P}$ versus the bifurcation parameter A. $t=0.1$ and $\sigma=0.01$.

We also assume that the random variables ξ_n in Eq. (1) obey the same normal (Gaussian) distribution with mean 0 and variance σ^2. In the following, we fix the value of parameter t at $t=0.1$ and consider that the other parameter A is the bifurcation parameter.

Figure 1 shows a deterministic bifurcation diagram of the map (7). A saddle-node bifurcation from quasiperiodic to period 1 occurs exactly at $A=0.10$ and the period-doubling bifurcations from period 1 to period 2 and from period 2 to period 4 occur near $A=0.334$ and $A=0.427$, respectively.

In the noisy case, note that the relation (6) always holds (if $\sigma>0$) since the noise considered here has a Gaussian distribution whose tail encircles the unit circle S infinitely. Thus the FP operator (matrix) $\mathcal{P}$ always has a unique (asymptotically stable) invariant density that is an eigenfunction of an eigenvalue 1 of the operator [9,11]. Thus the operator always has a real eigenvalue 1. It is also known that absolute values of the other eigenvalues of the operator are less than 1 [12]. Note that the eigenvalue with largest modulus other than 1 mainly governs the convergence speed of the sequence $\{h_n\}$ to the invariant density.

Examples of invariant density functions h^* and whole spectra (eigenvalues) of the operator $\mathcal{P}$ for various values of A are shown in Fig. 2. The density functions do not change their topological shapes around $A=0.10$ [see parts (a)–(d)], where a saddle-node bifurcation occurs in the deterministic case. So, we cannot see any stochastic bifurcations from quasiperiodic to period 1 in the classical sense. On the other hand, corresponding whole spectra changes much. Part (e) corresponds to the deterministic quasiperiodic case. Many complex eigenvalues whose moduli are very close to 1 are seen. Comparing, Figs. 2(f)–2(h), we can see that eigenvalues change their values from complex to real in the order of the modulus as the value of A increases.

Figure 3 is the ''spectral bifurcation diagram'' that shows the dependence of the eigenvalues on the parameter A. Parts (a) and (b) show the moduli and angles (arguments) of both the second and third (in the order of modulus) eigenvalues as a function of A. In the range of small A values, the eigenvalues are complex conjugate and become real slightly above the value $A=0.10$ that is a deterministic saddle-node bifurcation point. Parts (c) and (d) are the similar figures for the fourth and fifth eigenvalues and Figs. 3(e) and 3(f) for sixth and seventh ones. Although these figures show almost same branching behavior of eigenvalues in the case of second and third eigenvalues, we note that the branching points of smaller eigenvalues move rightwards slightly.

We have successfully defined a stochastic saddle-node bifurcation point as a point where the second eigenvalue becomes real number [11] (see Fig. 2). By the definition we can say that the saddle-node bifurcation point of the sine-circle map moves rightwards by imposing the additive Gaussian noise. Figure 4 shows the relation between the stochastic bifurcation points and the noise intensity σ, where stochastic bifurcation points are determined by the definition. The shift from the deterministic bifurcation point ($A=0.10$) is proportional to the noise intensity σ, which shows the validity of our definition. Note that all the invariant densities have the same topological shape and does not show any stochastic bifurcation in the classical sense.

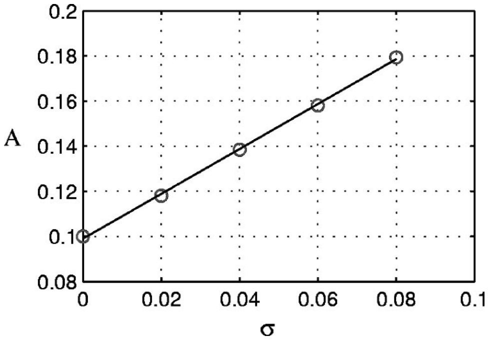

FIG. 4. Stochastic saddle-node bifurcation points versus the size of standard deviation σ. $t=0.1$. The line ($A=0.995\sigma+0.099$) is evaluated by using the four data and the deterministic bifurcation point ($A=0.10$).

IV. STOCHASTIC PERIOD-DOUBLING BIFURCATION

In this section we consider how stochastic periodicity is expressed in the eigenvalues and the eigenfunctions and how we can determine a period-doubling bifurcation point. Assume that λ_i denotes the ith eigenvalue in the order of modulus and u_i the corresponding eigenfunction. Now $\lambda_1=1$ and u_1 is an invariant density h^*. If we denote the eigenvalue as $\lambda_i=r_i e^{2\pi j\omega_i}$ with imaginary unit j, we have

$$\mathcal{P}^k u_i=\mathcal{P}^k(\mathrm{Re}\, u_i+j\,\mathrm{Im}\, u_i)=r_i^k e^{2\pi jk\omega_i}(\mathrm{Re}\, u_i+\mathrm{Im}\, u_i),$$

where $k=1,2,\ldots$. Thus we have

$$\mathcal{P}^k\,\mathrm{Re}\, u_i=r_i^k\{\cos(2\pi k\omega_i)\mathrm{Re}\, u_i-\sin(2\pi k\omega_i)\mathrm{Im}\, u_i\},$$

$$\mathcal{P}^k\,\mathrm{Im}\, u_i=r_i^k\{\cos(2\pi k\omega_i)\mathrm{Im}\, u_i+\sin(2\pi k\omega_i)\mathrm{Re}\, u_i\}.$$

If $k\omega_i$ is integer, both real and imaginary parts are invariant under $\mathcal{P}^k$ with an amplitude decay r_i^k. Therefore, stochastic periodicity with period k emerges if there exists a smallest integer k such that every $k\omega_i$ is integer for all i, or practically, for major eigenvalues.

Figure 5 corresponds to the deterministic period-doubling bifurcations from period 1 to period 2 and from period 2 to period 4. In the Figs. 5(a)–5(d), the peaks and the shape of the invariant density changes qualitatively. Correspondingly, the whole spectrum [Figs. 5(e)–5(h)] also changes much. A negative eigenvalue becomes the second largest (in the sense of absolute value) eigenvalue in the neighborhood of $A=0.25$ and the second largest eigenvalue is very close to -1 at $A=0.35$. At $A=0.35$, the whole spectrum is roughly invariant under an angle π rotation of complex plane that is a sign of period 2. At $A=0.40$, eigenvalues on imaginary axis become the third and the fourth largest eigenvalues. The second eigenvalue is still approximately -1 on the negative real axis. The moduli of the third and the fourth largest eigenvalues are close to 1 at $A=0.44$, where the whole spectrum is roughly invariant under an angle $\pi/2$ rotation of complex plane that is a sign of period 4.

Figure 6 is the spectral bifurcation diagram that shows the moduli and the angles of the second, third, fourth, and fifth eigenvalues of the operator $\mathcal{P}$ versus the bifurcation parameter A, where $A=[0.2,0.48]$. We can see that the angles of the major eigenvalues change their values discontinuously corresponding to the deterministic period-doubling bifurcation. The angle of the second eigenvalue changes from 0 to π near $A=0.25$, which corresponds to the deterministic bifurcation to period 2. This discontinuous change appears because the replacement of the second largest eigenvalue occurs at the point, where the modulus of the third eigenvalue on the negative real axis becomes the second largest [see, Fig. 5(e)]. We also see that the angles of the third and the fourth eigenvalues become $\pi/2$ and $3\pi/2$ discontinuously near $A=0.40$, which correspond to the deterministic bifurcation to period 4. Moduli of the eigenvalues also change their values corresponding to the deterministic period-doubling bifurcation.

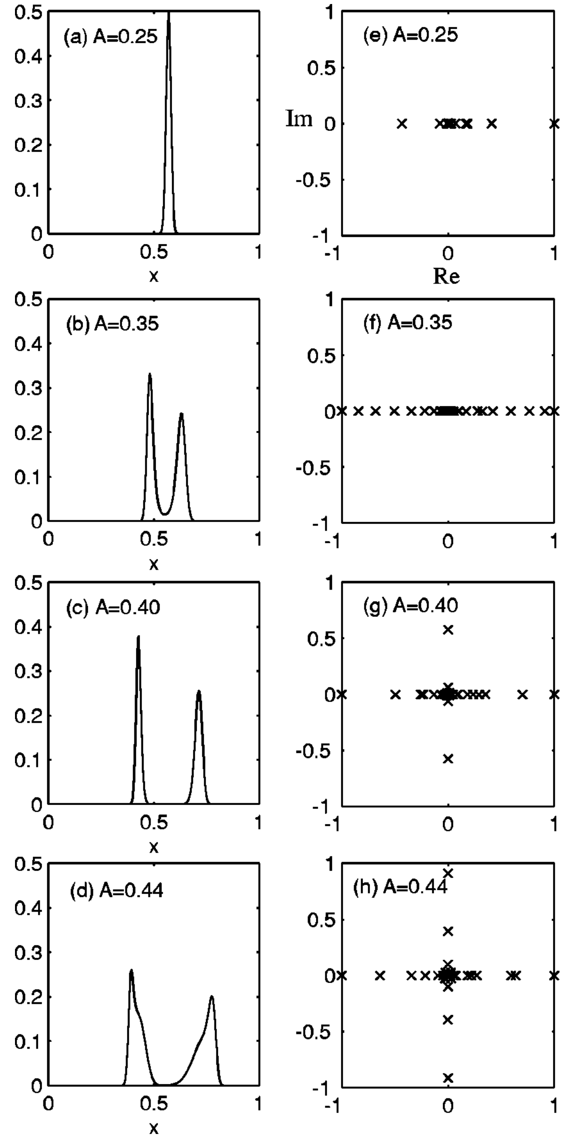

FIG. 5. Stochastic period-doubling bifurcation. Same figure as Fig. 2. In the deterministic case, period-doubling bifurcations from period 1 to period 2 and from period 2 to period 4 occur near $A=0.334$ and $A=0.427$, respectively.

We might say that the point where the angle of the second eigenvalue changes from 0 to π is a stochastic bifurcation

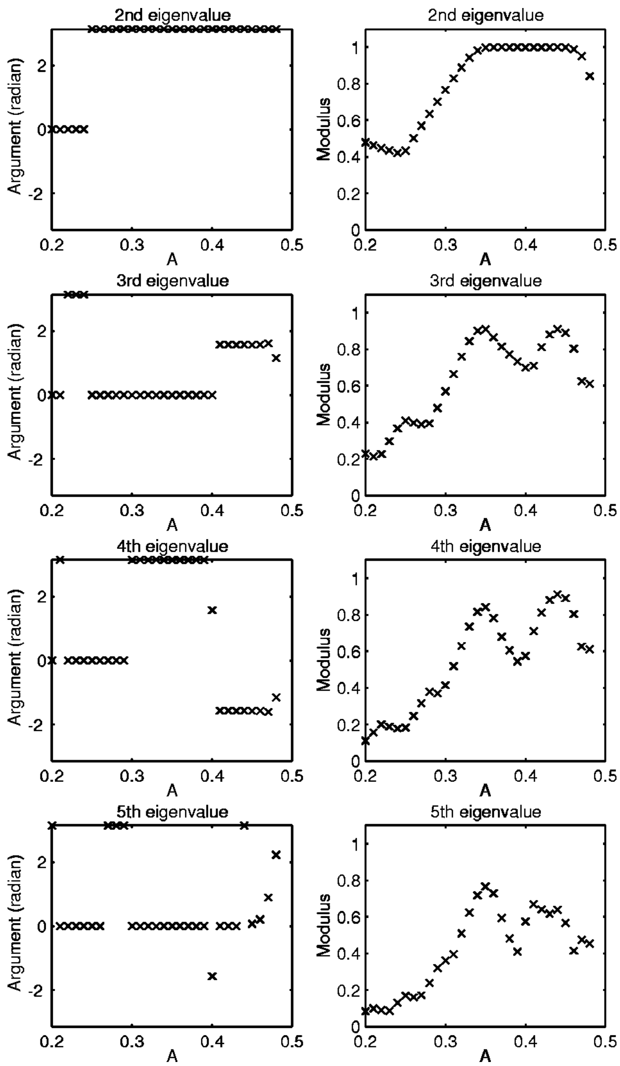

FIG. 6. Spectral bifurcation diagram (period-doubling bifurcation). Moduli and angles of the second, third, fourth, and fifth eigenvalues of the operator $\mathcal{P}$ versus the bifurcation parameter A. $t = 0.1$ and $\sigma = 0.01$.

point from period 1 to period 2 and the point where the angle of the third and the fourth eigenvalues change to $\pi/2$ and $3\pi/2$ is a stochastic bifurcation point from period 2 to period 4. The relation between the shift of bifurcation points and the size of standard deviation σ of additive noise are plotted in Fig. 7, where stochastic bifurcation points are determined by using the definitions that are stated above. In the case of saddle-node bifurcation the shift from the deterministic bifurcation point is proportional to the noise size σ. On the other hand, the shift increases as the noise size σ decreases to 0 in the period-doubling case. This relation is very strange and suggests that the definition for period-doubling bifurcation is not adequate.

Another candidate of the bifurcation point could be the point where the second eigenvalue becomes very close to unity in the case of the bifurcation from period 1 to period 2, because the speed of the convergence to the invariant density is very slow at the point. Figure 8 shows moduli of the eigenvalues of the operator $\mathcal{P}$ versus the bifurcation parameter

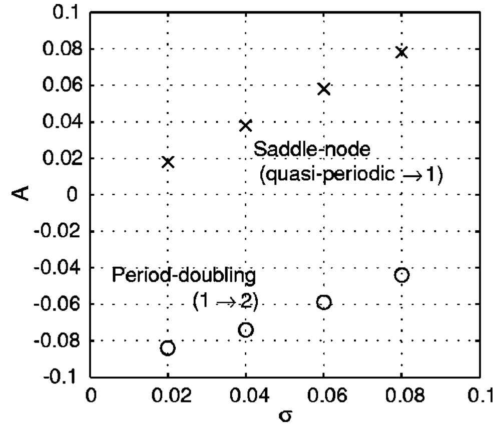

FIG. 7. The relation between the shift of bifurcation points and the size of standard deviation σ. $\sigma = 0.02$, 0.04, 0.06, 0.08. Multiplies: bifurcation point from quasiperiodic to period 1. Circles: bifurcation point from period 1 to period 2. $t = 0.01$.

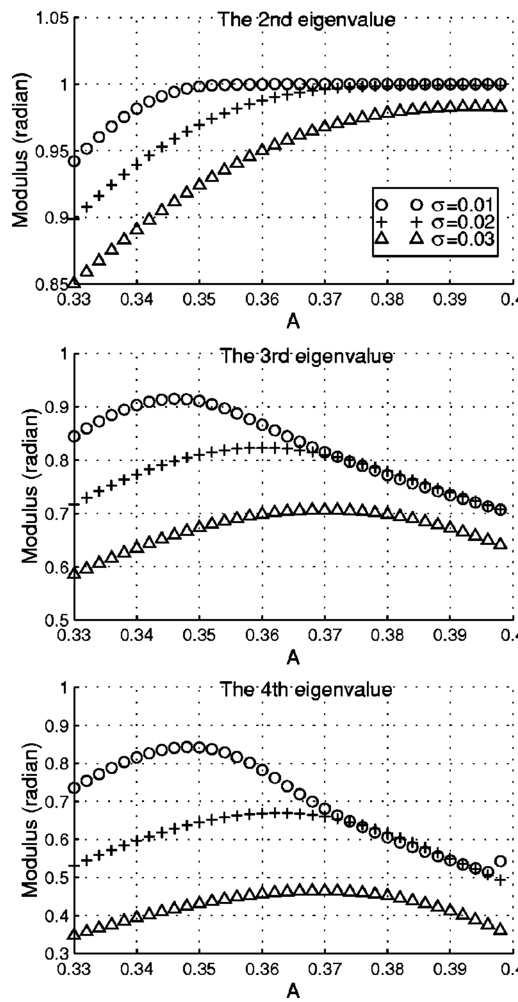

FIG. 8. Moduli of the eigenvalues of the operator $\mathcal{P}$ versus the bifurcation parameter A with different noise intensities σ in the case of the period-doubling bifurcation. $t = 0.1$, $\sigma = 0.01$, 0.02, 0.03.

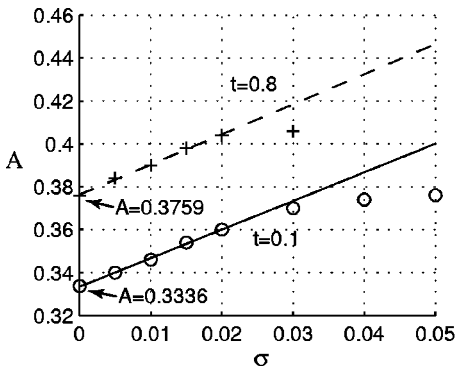

FIG. 9. Stochastic period-doubling bifurcation points versus the size of standard deviation σ. The abscissa is the size of σ and the ordinate is the bifurcation points. Circles: the case of the map parameter $t=0.1$. Plusses: $t=0.8$. Lines are evaluated, respectively, by using the first four data and the deterministic bifurcation points calculated analytically. The broken line is $A=1.40\sigma+0.376$. The solid line is $A=1.33\sigma+0.333$.

A with different noise intensities σ. Since the second eigenvalues gradually increase to unity, it is not easy to tell at which value of the parameter A the eigenvalue becomes very close to unity.

On the other hand, the third and the forth eigenvalues take their maximum values in this range of A, see Fig. 8. Furthermore, the second eigenvalues become very close to unity at the value of A where the third eigenvalues become maximum. Thus let us define that the value of A where the third eigenvalue takes it maximum is a bifurcation point of a period doubling from period 1 to period 2. In Fig. 9, bifurcation points in the sense of this definition are plotted with different size σ of standard deviation. Similar plots are also obtained in the case of the map parameter $t=0.8$. As is easily seem in the figure, the stochastic period-doubling bifurcation point shifts rightward as the noise intensity increases and the amount of the shift is proportional to the noise intensity σ when σ is small. Therefore, it may safely be defined that the value of A where the third eigenvalue takes it maximum is a bifurcation point of the period doubling from period 1 to period 2.

V. DISCUSSION

We have analyzed both stochastic saddle-node and period-doubling bifurcations in a noisy one-dimensional mapping. The analysis method uses spectra (eigenvalues and eigenfunctions) of the FP operator that governs the probability density evolution of the system and detects a stochastic bifurcation point as a point where some characteristics of specific spectra change. This method enables us to quantitatively study very delicate phenomena caused by noise without heavy numerical (Monte Carlo) simulations.

We have demonstrated and verified numerically our method by using a noisy sine-circle mapping that shows both saddle-node bifurcations and period-doubling bifurcations. Stochastic saddle-node bifurcation has been successfully described by the identical definition with the one used in the previous study [11]. Stochastic period-doubling bifurcations were clearly observed in terms of the FP operator of the system.

We would like to emphasize that the method that uses the FP operator enables us to discuss stochastic bifurcations quantitatively. In fact, we were able to discuss the relation between the shift of bifurcation points from the corresponding deterministic ones and the noise intensity σ, which is an example of the quantitative study. The relations are linear when σ is small in case of both the saddle-node bifurcation and the period-doubling bifurcation (see Figs. 4 and 9). It is worth pointing out that the slopes of the lines in Fig. 9 are much larger than the one in Figs. 4, which may show the high sensitivity of the period-doubling bifurcation against noise.

Needless to say, the validity of our definition for the stochastic period-doubling bifurcation point is still open to debate. A more rigorous discussion on the validity of our definition is necessary for future research.

The FP operator has been discretized as an $n\times n$ matrix where we mainly treated the case of $n=200$ in this paper. If we increase the discretization size, eigenvalues with larger absolute values do not change much but smaller eigenvalues do change; the number of eigenvalues with nearly zero absolute value increases. This means that zero is the accumulation point of eigenvalues of the FP operator. If the standard deviation of noise is small or the deterministic map is totally superstable (the slope of the map is close to zero as a whole), the discretization error becomes relatively large; in such cases we need a larger discretization size to get eigenvalues of desirable precision.

ACKNOWLEDGMENTS

This research was partially supported by the Japanese Ministry of Education, Science, Sports, and Culture, Grant-in-Aid (No. 10650429 and No. 10780248).

[1] P. Collet and J.P. Eckmann, *Iterated Maps on the Interval as Dynamical Systems* (Birkhäuser, Boston, 1980).

[2] W. de Melo and S. van Strien, *One-Dimensional Dynamics* (Springer, Berlin, 1993).

[3] G. Mayer-Kress and H. Haken, J. Stat. Phys. **26**, 149 (1981).

[4] J.P. Crutchfield, J.D. Farmer, and B.A. Huberman, Phys. Rep. **92**, 45 (1982).

[5] S. Doi, J. Stat. Phys. **55**, 941 (1989).

[6] W. Horsthemke and R. Lefever, *Noise-Induced Transitions, Theory and Applications in Physics, Chemistry, and Biology* (Springer-Verlag, Berlin, 1984).

[7] T. Kapitaniak, *Chaos in systems with noise* (World Scientific, Singapore, 1988).

[8] *Noise in Nonlinear Dynamical Systems*, edited by F. Moss and P.V.E. McClintock (Cambridge University Press, Cambridge, 1987), Vols. 1-3.

[9] A. Lasota and M. C. Mackey, *Chaos, Fractals, and Noise: Stochastic Aspects of Dynamics* (Springer, Berlin, 1994).

[10] L. Arnold, *Random Dynamical Systems* (Springer, Berlin, 1998).

[11] S. Doi, J. Inoue, and S. Kumagai, J. Stat. Phys. **90**, 1107 (1998).

[12] S.-J. Chang and J. Wright, Phys. Rev. A **23**, 1419 (1981).

[13] R. Badii and A. Politi, *Complexity: Hierarchical Structures and Scaling in Physics*, Cambridge Nonlinear Science Series 6 (Cambridge University Press, Cambridge, 1997).